Thin Solid Films 517 (2009) 2767–2774

Contents lists available at ScienceDirect

Thin Solid Films

journal homepage: www.elsevier.com/locate/tsf

Effect of $LaNiO_3$ electrodes and lead oxide excess on chemical solution deposition derived $Pb(Zr_x,Ti_{1-x})O_3$ films

Itzik Shturman, Gennady E. Shter, Aleksey Etin, Gideon S. Grader *

Chemical Engineering Department, Technion, Haifa 32000, Israel

ARTICLE INFO

Article history:
Received 22 September 2007
Received in revised form 26 August 2008
Accepted 5 October 2008
Available online 15 October 2008

Keywords:
$LaNiO_3$ (LNO)
$Pb(Zr_x,Ti_{1-x})O_3$ (PZT)
Chemical solution deposition (CSD)

ABSTRACT

The effects of $LaNiO_3$ (LNO) and Pt electrodes on the properties of $Pb(Zr_x,Ti_{1-x})O_3$ (PZT) films were compared. Both LNO and PZT were prepared by chemical solution deposition (CSD) methods. Specifically, the microstructure of LNO and its influence on the PZT properties were studied as a function of PbO excess. Conditions to minimize the Pyrochlore phase and porosity were found. Remnant polarization, coercive field and fatigue limit were improved in the PZT/LNO films relative to the PZT/Pt films. Additionally, the PZT crystallization temperature over LNO was 500 °C, about ~50 °C lower than over Pt. The crystallization temperature reported here is amongst the lowest values for CSD-based PZT films.

1. Introduction

Thin $PbZr_xTi_{1-x}O_3$ (PZT) films have excellent ferroelectric and piezoelectric properties which make them useful for sensors, actuators and memory applications [1–4]. Pt is often integrated as an electrode in PZT devices because of its stability at high temperature, low leakage current and high electrical conductivity [5]. However, in addition to its high cost, Pt has several disadvantages such as poor adhesion to the silicon substrate and a large thermal expansion coefficient mismatch with PZT. The poor adhesion is typically solved by deposition of a Ti intermediate adhesion layer. The main disadvantage of PZT/Pt device is the low ferroelectric fatigue limit that causes a severe decrease in the ferroelectric properties after 10^4–10^7 operating cycles [3,6,7]. The two main reasons for the fast fatigue in PZT/Pt system are thought to be: formation of oxygen vacancies in the PZT films during operation cycles [7,8] and the presence of Pyrochlore (Py) phase [3] that pinned the domain switching.

Lanthanum nickel oxide (LNO) is a conducting oxide film which has attracted great attention in recent years due to its ability to drastically improve the ferroelectric fatigue [7,9] of PZT. LNO has lattice parameter of 0.384 nm and its typical film resistivity at room temperature is in the 300 μΩ*cm to 2000 μΩ*cm range [10]. Furthermore, LNO structure is compatible with PZT, since both have perovskite ABO_3 type unit cell [6] with 0.384 nm and 0.404 nm lattice constant for LNO and PZT respectively. Hence, LNO is an excellent candidate in coupling with PZT devices. The remnant polarization (Pr) and coercive field (Ec) of PZT/LNO have been reported to improve in comparison with PZT/Pt system. It was suggested that the improved ferroelectric properties were due to better PZT interface with LNO electrodes in comparison with Pt [11] electrodes.

LNO electrodes can be made by different techniques such as pulsed laser ablation [12], r.f. magnetron sputtering [6], and chemical solution deposition (CSD) methods that include metalorganic decomposition [13] as well as the Sol-Gel route [14]. The CSD method offers several advantages over other routes such as easy elemental stoichiometry control which is critical in multi-component ceramic systems, low process costs and high throughput. Only few reports have been made on a complete CSD approach [15,16], (for both bottom electrode and PZT films), and the analysis of the morphology and ferroelectric properties is still partially investigated. Specifically, the influence of PbO content on morphology and ferroelectric properties in PZT/LNO has not been reported yet.

In the present research both LNO and PZT were prepared by CSD, and results compared with those obtained with Pt bottom electrodes. The microstructure and electrical properties of LNO electrodes and their influence on PZT morphology, orientation and ferroelectric behavior were studied as a function of PbO excess.

2. Experimental details

LNO electrodes were prepared using the CSD method. Solution precursors were prepared by dissolving lanthanum acetate hydrate $C_6H_9LaO_6{\cdot}xH_2O$ (99.9%, Sigma-Aldrich, Steinheim, Germany) in a mixture of distilled water and glacial acetic acid $C_2H_4O_2$ (99.8%, Gadot, Netanya, Israel) in a molar ratio of 1:15:144 for lanthanum acetate hydrate, distilled water and glacial acetic acid respectively at 75 °C for 1 h. An equi-molar amount of nickel acetate tetrahydrate (98% Sigma-Aldrich) was dissolved in glacial acetic acid in a molar ratio of 1:25 for

* Corresponding author. Tel.: +972 4 8292008; fax: +972 4 8295672.
E-mail address: grader@techunix.technion.ac.il (G.S. Grader).

0040-6090/$ – see front matter © 2008 Elsevier B.V. All rights reserved.
doi:10.1016/j.tsf.2008.10.007

nickel acetate tetrahydrate and acetic acid respectively at 75 °C for 1 h. These solutions were stirred together at 75 °C for 1 h. The green final precursor's concentration was 0.2 M and it's assay was 4.5% wt. The precursor had a shelf life of more than one year without any visual phase separation and without any changes in the final electrode properties. LNO electrodes were prepared by spin coating at 3000 rpm for 60 s, acceleration of 1000 rpm/s, followed by pyrolysis on a hot plate at 350 °C for 2 min and a final annealing step at 700 °C for 20 min in Air. Due to the relatively low concentration of the LNO precursor, the resulting film thickness per cycle was ~25 nm. The deposition cycle was repeated till the desired LNO thickness in the range of 25–225 nm was achieved.

The detailed preparation of the PZT precursors and films is described elsewhere [2–4]. In the present work PZT precursors of with 10% and 30% PbO excess were prepared and diluted with 1-octanol in order to deposit defect-free PZT films [4]. The CSD route for PZT deposition over LNO and Pt electrodes was as follows: 3 cycles of spinning at 3000 rpm for 1 min with acceleration of 1000 rpm/s, pyrolysis on a hot-plate at 300 °C for 1 min, and a final annealing step at 650–500 °C in air for 10–60 min. Upper Au circular electrodes (500 μm diameter), were deposited by evaporation (Edwards E306A, Crawley, UK), using a contact mask technique. The film surface and cross-sectional microstructure were studied with a high-resolution field emission gun equipped with a scanning electron microscope (LEO 982, Cambridge, U.K). Conditions included a 4 kV accelerating voltage and a 4 to 5 mm working distance, using an in-lens detector of secondary electrons. The grain size was determined by the equivalent area method without a correction factor using an image analysis software (Image tool, Copyright UTHSCSA) based on the HRSEM pictures. In order to enhance the grain boundary definition, the nanoparticles were analyzed when image is viewed in the threshold mode. Only particles with well-defined boundaries were considered as individual grains.

The crystalline phases were detected by X-ray diffraction (XRD), using a Siemens D5000 powder diffractometer instrument (Siemens, Karlsruhe , Germany). Atomic force microscopy (AFM) analyses were performed at scanning area of 2.5×2.5 μm^2 in a non-contact mode using an Agilent 5500 system (Tempe, USA). For the LNO electrode resistivity measurements a four point probe method was used with Veeco FPP5000 system (Tucson, USA) and a distance of 1.59 mm between the probe tips. An elemental distribution depth profile in the LNO film was obtained with secondary ion mass spectrometer, SIMS (Cameca ims-4 f, Paris, France). The sample was sputtered using a 3 keV Cs+ primary ions source by monitoring O, Si, Ni, La, Ti, Zr and Pb secondary ions from a 40 μm^2 area. The fatigue and hysteresis measurements were tested using a Sawyer–Tower bridge. The applied voltage was a 15 V (peak to peak) sine wave with a 1 kHz or 10 kHz frequency for hysteresis and fatigue measurements, respectively.

3. Results and discussion

3.1. Film morphology and resistivity

The surface morphology of LNO electrodes with different thickness are shown in Fig. 1a-c. It can be seen that the size of the LNO grains increases with the thickness. As shown in Fig. 1d, the average LNO grain size is 38 nm and 58 nm for electrode thickness of 75 nm and 225 nm, respectively. For defect-free bulk materials, the grain size (D), is typically proportional to the square root of annealing time [17] (i.e. $D \alpha t^{0.5}$). Our experimental results indicate that for LNO electrode the grain size is proportional to 0.4 power of the thickness (Fig. 1d). The shift in the power value in comparison with the literature [17] can be explained by two factors: the experimental value is based on an LNO film rather than bulk, and the film is probably not defect free. Defects can pin the grain growth and lead to a smaller than expected grain

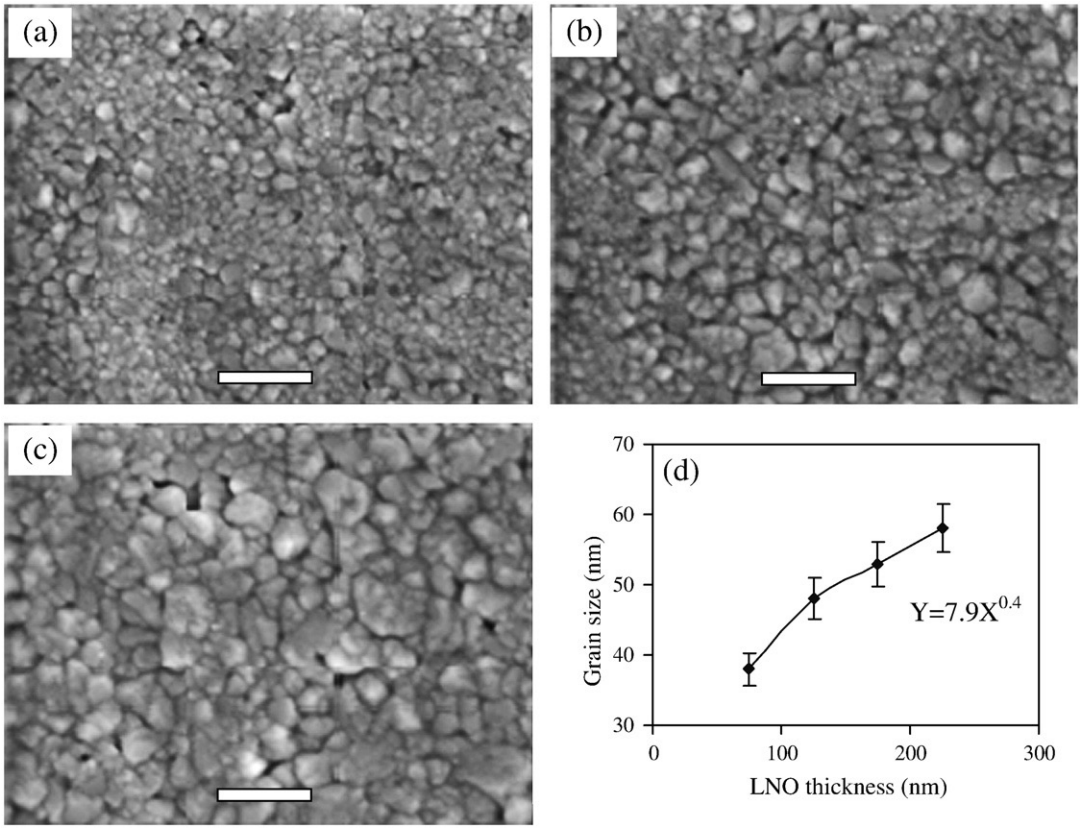

Fig. 1. HRSEM film morphology of LNO at thickness of (a) 75 nm, (b) 125 nm, (c) 225 nm and (d) grain size vs. thickness; bar-200 nm.